



Consistent increase in dimethyl sulfide (DMS) in response to high CO₂ in five shipboard bioassays from contrasting NW European waters

F. E. Hopkins¹ and S. D. Archer^{1,*}

¹Plymouth Marine Laboratory, Plymouth, UK

* now at: Bigelow Laboratory for Ocean Sciences, Maine, USA

Correspondence to: F. E. Hopkins (fhop@pml.ac.uk)

Received: 31 December 2013 – Published in Biogeosciences Discuss.: 10 February 2014

Revised: 25 July 2014 – Accepted: 5 August 2014 – Published: 16 September 2014

Abstract. The ubiquitous marine trace gas dimethyl sulfide (DMS) comprises the greatest natural source of sulfur to the atmosphere and is a key player in atmospheric chemistry and climate. We explore the short-term response of DMS production and cycling and that of its algal precursor dimethyl sulfoniopropionate (DMSP) to elevated carbon dioxide (CO₂) and ocean acidification (OA) in five 96 h shipboard bioassay experiments. Experiments were performed in June and July 2011, using water collected from contrasting sites in NW European waters (Outer Hebrides, Irish Sea, Bay of Biscay, North Sea). Concentrations of DMS and DMSP, alongside rates of DMSP synthesis and DMS production and consumption, were determined during all experiments for ambient CO₂ and three high-CO₂ treatments (550, 750, 1000 μatm). In general, the response to OA throughout this region showed little variation, despite encompassing a range of biological and biogeochemical conditions. We observed consistent and marked increases in DMS concentrations relative to ambient controls (110 % (28–223 %) at 550 μatm, 153 % (56–295 %) at 750 μatm and 225 % (79–413 %) at 1000 μatm), and decreases in DMSP concentrations (28 % (18–40 %) at 550 μatm, 44 % (18–64 %) at 750 μatm and 52 % (24–72 %) at 1000 μatm). Significant decreases in DMSP synthesis rate constants (μDMSP, d⁻¹) and DMSP production rates (nmol d⁻¹) were observed in two experiments (7–90 % decrease), whilst the response under high CO₂ from the remaining experiments was generally indistinguishable from ambient controls. Rates of bacterial DMS gross consumption and production gave weak and inconsistent responses to high CO₂. The variables and rates we report increase

our understanding of the processes behind the response to OA. This could provide the opportunity to improve upon mesocosm-derived empirical modelling relationships and to move towards a mechanistic approach for predicting future DMS concentrations.

1 Introduction

Dimethyl sulfide (DMS) is a ubiquitous marine trace gas derived from the breakdown of the algal osmolyte β-dimethyl sulfoniopropionate (DMSP). A variety of phytoplankton species produce DMSP, with the majority of production attributed to prymnesiophytes, dinoflagellates and diatoms (Stefels, 2000). Reasons for algal biosynthesis of DMSP are thought to include its role as an overflow product for the regulation of carbon and sulfur metabolism, as an osmolyte or compatible solute, and as defence mechanism against microbes, viruses and zooplankton grazing. Finally, along with its breakdown products (DMS, acrylate, dimethyl sulfoxide (DMSO)), DMSP scavenges harmful hydroxyl radicals and other reactive oxygen species, potentially providing the cell with antioxidant protection (Sunda et al., 2002, 2007).

DMSP is released from phytoplankton cells into the dissolved phase by active exudation or when cells are lysed during grazing, viral attack or senescence (Stefels et al., 2007). Once in this phase, marine bacteria play a vital role in the fate of DMSP in the surface oceans. Indeed, most DMSP released from phytoplankton is either catabolised by bacteria to produce DMS (Todd et al., 2007, 2009), or

demethylated/demethiolated to produce other key organosulfur compounds such as methanethiol (MeSH) (Kiene et al., 2000; Moran et al., 2012). The demethylation/demethiolation (de/de) pathway regularly dominates as it is considered more energetically advantageous than the cleavage pathway (Kiene et al., 2000; Simó et al., 2002; Moran et al., 2012). Thus, DMSP turnover often exceeds DMS production in the surface oceans. However, the factors regulating the switch between these two competing pathways are still poorly understood (Moran et al., 2012).

DMS is also subject to rapid biological consumption, a process thought to account for 50–80 % of total DMS loss in the surface oceans and one which often dominates in bloom situations (Gabric et al., 1999; Simó, 2004). Photochemical loss of DMS competes with this biological loss pathway, comprising a comparable proportion of the total loss (Toole et al., 2006; Vila-Costa et al., 2008). Of the total DMSP produced in the oceans, only ~1 % remains to undergo exchange to the atmosphere – however this flux, amounting to ~28 Tg S yr⁻¹, comprises approximately 50 % of the total global natural S flux (Andreae, 1990; Lana et al., 2011). In the atmosphere, DMS is rapidly oxidised, forming oxidation products that contribute to the atmospheric aerosol burden, and can lead to the formation and/or growth of particles (Charlson et al., 1987; Barnes et al., 2006). In addition, DMS-derived aerosols are highly effective at influencing cloud albedo, with implications for global radiative forcing (Rap et al., 2013).

Increasing atmospheric CO₂ levels and the corresponding oceanic uptake of excess CO₂ is resulting in changes to the carbonate chemistry of the surface oceans. This process, termed ocean acidification (OA), manifests itself as decreasing carbonate ion concentrations [CO₃²⁻], increasing hydrogen ion concentrations [H⁺] and a corresponding decrease in seawater pH (Caldeira and Wickett, 2003). Since industrialisation, mean surface ocean pH has fallen by 0.1 pH units. A further decrease of 0.4–0.5 pH units by 2100 is likely unless stringent global CO₂ emissions stabilisation is implemented (Caldeira and Wickett, 2003, 2005). Such rapid changes to seawater chemistry, potentially unprecedented in the last ~300 Ma, are likely to have serious repercussions for marine biological and biogeochemical processes (Raven et al., 2005; Hendriks et al., 2010; Liu et al., 2010; Riebesell and Tortell, 2011; Hönisch et al., 2012).

The majority of OA experiments that consider DMS/DMSP have been coastal temperate and subpolar mesocosms, with observations of bulk DMS and DMSP made over 3–4 weeks during a nutrient-induced springtime phytoplankton bloom (Wingenter et al., 2007; Vogt et al., 2008; Hopkins et al., 2010; Kim et al., 2010; Avgoustidi et al., 2012; Archer et al., 2013). Thus, available data are limited by lack of geographical and seasonal coverage. Decreases in DMS have been observed under predicted turn-of-the-century (year 2100) levels of CO₂, ranging from ~35 % (Archer et al., 2013) to ~60 % (Hopkins

et al., 2010; Avgoustidi et al., 2012) relative to ambient controls. When similar levels of pH-driven changes in DMS concentrations are applied globally, the resultant changes in DMS emissions from the oceans may be sufficiently large to influence climate (Six et al., 2013). However, the pattern of decreasing DMS with decreased pH is not consistent amongst all mesocosm experiments. The study by Kim et al. (2010) reported a ~80 % increase in DMS under high CO₂. In one case, little difference in concentrations between ambient and high CO₂ was observed (Vogt et al., 2008). The DMSP response is similarly variable but of comparable orders of magnitude. Simple relationships have been derived with biological measurements (e.g. plankton community structure, pigments, bacterial abundance and rates) as drivers of the observed DMS and DMSP responses. Physiological effects at the cellular level are more difficult to detect. Broad community-level taxonomic shifts drive the DMS response because the altered conditions favour some species over others (Engel et al., 2008; Meakin and Wyman, 2011; Newbold et al., 2012; Brussaard et al., 2013). Besides the mesocosm experiments, one past study reported the response of natural communities using a shipboard continuous culture system (Lee et al., 2009); here, elevated CO₂ had no effect on concentrations of DMSP. There is still a fundamental lack of mechanistic and physiological understanding of the responses and limited information on regional variability.

Improved predictive capability of models is likely to require a better understanding of the mechanisms driving OA-induced changes in DMS biogeochemistry. Unialgal cultures potentially provide a useful insight into the specific physiological response of a single species to elevated CO₂. DMS decreased two- to tenfold in cultures of the coccolithophore *Emiliania huxleyi* under high CO₂ (Arnold et al., 2013; Avgoustidi et al., 2012), whereas intracellular DMSP responded differently, with both significant decreases (Avgoustidi et al., 2012) and increases (Arnold et al., 2013). Spielmeyer and Pohnert (2012) reported decreases in cellular DMSP in diatoms, but increases in non-calcifying strains of *E. huxleyi*. How informative these results are with regard to the complex DMSP and DMS cycle in natural communities is questionable.

In an attempt to bridge the gap between the complexity of interpreting processes in traditional mesocosm experiments and the limited applicability of unialgal culture experiments to natural systems, this study was designed to assess the eco-physiological response of a variety of natural microbial communities from a wide geographic area to high CO₂. Detailed discussion of the choice of experimental design in the context of previous OA studies is given in this issue by Richier et al. (2014a). By determining rates of key processes, along with standing stock measurements of DMSP and DMS, we can consider a number of hypotheses. Firstly, increased CO₂ may stimulate primary productivity in phytoplankton communities (Riebesell and Tortell, 2011), resulting in enhanced DMSP synthesis rates and increased DMSP concentrations

(Archer et al., 2013). Secondly, elevated primary production may stimulate bacterial production by increasing the availability of organic substrates (Weinbauer et al., 2011; Engel et al., 2013; Piontek et al., 2013). This would create a greater bacterial demand for DMSP sulfur and stimulate the de/de pathway, whilst also resulting in an increase in bacterial DMS consumption. The overall effect would be decreased gross DMS production.

2 Materials and methods

2.1 Experimental bioassays

Five shipboard experimental bioassays (hereafter E01–E05) were undertaken during the UK Ocean Acidification Research Programme (UKOA) NW European shelf cruise aboard the RRS Discovery from 6 June to 10 July 2011. Full details of the sampling and experimental setup are given elsewhere in this issue by Richier et al. (2014a), and a general overview is given here; all data are available from the British Oceanographic Data Centre (Richier et al., 2014b). For bioassay water collection, a stainless steel conductivity–temperature–depth (CTD) rosette comprising twenty-four 20 L bottles was deployed, and all bottles were simultaneously fired at the near surface (5–12 m). Water collection commenced pre-dawn, at 02:00 GMT for E01–E04 and at 01:00 GMT for E05 due to its more northerly location and earlier sunrise time (locations and sample depths given in Fig. 1 and Table 1). Once the rosette was back on deck, the water was directly transferred into 4 L polycarbonate bottles, with no screening or filtration. Manipulations of the carbonate chemistry were achieved by additions of NaHCO_3^- (1 M) and HCl (1 M) to attain the four target CO_2 levels (ambient, 550 μatm , 750 μatm , 1000 μatm). After first ensuring the absence of bubbles or headspace, the bottles were sealed with septa lids (high-density polyethylene (HDPE) with silicone and polytetrafluoroethylene (PTFE) septum) and placed in the incubation container. Bottles were incubated inside a custom designed temperature- and light-controlled shipping container, set to match the in situ water temperature at the time of collection. A constant light level ($100 \mu\text{E m}^{-2} \text{s}^{-1}$) incorporating an 18–6 h light–dark cycle was provided by daylight simulation LED panels (Powerpax, UK). The daily light dose within the experimental bioassays was considered to be as close to representative as possible of that experienced in situ by the microbial community. Details of the integrated mixed layer irradiances at the time of sample collection for each experiment are given in Richier et al. (2014a). Each bottle belonged to a set of biological triplicates, and sacrificial sampling of bottles was performed at one of two time points (T1 at 48 h and T2 at 96 h), with three sets of biological triplicates for each time point to allow for the sampling requirements of the entire scientific party (3×3 bottles, $\times 2$ time points, $\times 4 \text{CO}_2$ treatments = 72 total). At each

time point (48 h and 96 h), the relevant bottles were removed from the incubation container and sampled. Samples for carbonate chemistry measurements were made first to avoid gas exchange with ambient air, followed by sampling for DMS, DMSP and related parameters.

2.2 DMS and DMSP standing stocks

The volume of water required to fill all experimental bioassay bottles and to make key initial measurements (carbonate chemistry, nutrients, Chl *a*, photophysiology) was such that there was insufficient water for DMS-related initial measurements to be taken from the same CTD cast. Therefore, a second CTD cast was carried out after the bioassay cast to collect additional water for further initial measurements, at the same station and depth, 2–3 h after the primary bioassay cast. Carbonate chemistry parameters (dissolved inorganic carbon (DIC), total alkalinity (TA), pH, $p\text{CO}_2$; see Richier et al. (2014a) for details of methods) were determined from both 0 h bioassay bottles and the second CTD cast. Single values from bioassay 0 h bottles fell within the range of triplicate values from 0 h CTD casts (Table S1 in the Supplement), suggesting little or no change in water mass between CTD casts. It was from these additional CTD casts that all initial DMS and DMSP samples were taken. Samples were taken directly from the Niskin bottles using Tygon tubing and collected in 250 mL amber glass-stoppered bottles. The bottle was rinsed three times before being filled gently from the bottom and then allowed to overflow three times. Once full, the glass stopper was securely placed on the bottle, ensuring the presence of no headspace. Samples were kept in a cool box and analysed within 2 h.

Samples at experimental time points (48 h, 96 h) were taken directly from the bioassay bottles. After inverting the bioassay bottle three times to ensure resuspension of particulates, samples were siphoned from the bottles directly into 100 mL glass-stoppered bottles using 6 mm silicone tubing. The bottle was first rinsed then filled to the top, ensuring the presence of no bubbles or headspace.

Seawater DMS concentrations were determined by cryogenic purge and trap, followed by detection via gas chromatography with a pulsed flame photometric detector, as outlined in Archer et al. (2013). Total DMSP concentrations (DMSPt) from the same sample bottle were fixed by the addition of 35 μL of 50 % H_2SO_4 to 7 mL of seawater (Kiene and Slezak, 2006) and analysed within 2 months of collection, again as described in Archer et al. (2013). DMS calibrations were performed using alkaline cold hydrolysis (10 M NaOH) of DMSP (>98 % purity, Centrum voor Analyse, Spectroscopie and Synthese, Rijksuniversiteit Groningen) diluted 3 times in Milli-Q water to give working standards in the range 0.03–3.3 ng S mL^{-1} , and multi-point calibrations were performed every 2–4 days throughout the cruise.

Table 1. Overview of initial conditions for experimental bioassays. MLD stands for mixed layer depth, DMSPt is total DMSP and DMSPP is particulate DMSP. Data shown are means (\pm standard error) for triplicate measurements made at 0 h for each experiment. Standard errors are not shown for experimental $p\text{CO}_2$ and pH as values are based on single measurements.

	E01	E02	E03	E04	E05
	56°47.688 N	52°28.237 N	46°12.137 N	52°59.661 N	56°30.293 N
	7°24.300 W	5°54.052 W	7°13.253 W	2°29.841 E	3°39.506 E
	Mingulay Reef	Irish Sea	Bay of Biscay	S North Sea	Mid North Sea
	8 June 2011	14 June 2011	21 June 2011	26 June 2011	2 July 2011
Regime	Stratified	Mixed	Stratified	Mixed	Stratified
Sample depth (m)	6	5	10	5	12
MLD (total depth) (m)	13 (190)	76 (76)	44 (4760)	33 (33)	14 (72)
T ($^{\circ}\text{C}$)	11.3	11.8	15.3	14.6	14.0
Salinity	34.8	34.4	35.8	34.1	35.0
$p\text{CO}_2$ (μatm)					
In situ	342.6 \pm 2.4	333.7 \pm 3.1	339.8 \pm 3.5	400.6 \pm 3.3	368.1 \pm 2.5
Ambient	342.3	no data	345.4	395.4	374.7
~ 550	564.1	533.4	531.2	533.4	528.9
~ 750	746.4	no data	674.0	691.4	730.5
~ 1000	969.6	862.7	877.8	936.6	917.5
pH					
In situ	8.11 \pm 0.003	8.11 \pm 0.004	8.12 \pm 0.004	8.05 \pm 0.003	8.07 \pm 0.003
Ambient	8.10	no data	8.10	8.05	8.07
~ 550	7.91	7.94	7.95	7.94	7.94
~ 750	7.80	no data	7.85	7.84	7.82
~ 1000	7.70	7.75	7.75	7.72	7.73
Nutrients and Chl a					
NO_3^- (μM)	1.1 \pm 0.1	0.3 \pm 0.01	0.6 \pm 0.0	0.9 \pm 0.14	0.21 \pm 0.04
$\text{Si}(\text{OH})_4$ (μM)	2.1 \pm 0.04	0.5 \pm 0.01	0.6 \pm 0.01	0.8 \pm 0.01	0.1 \pm 0.01
PO_4^{3-} (μM)	0.1 \pm 0.2	0.1 \pm 0.01	0.1 \pm 0.001	0.1 \pm 0.01	0.04 \pm 0.01
Total Chl a ($\mu\text{g L}^{-1}$)	3.3 \pm 0.04	3.5 \pm 0.07	0.8 \pm 0.04	1.3 \pm 0.03	0.3 \pm 0.01
> 10 μm Chl a ($\mu\text{g L}^{-1}$)	no data	2.8 \pm 0.12	0.3 \pm 0.02	0.3 \pm 0.03	0.1 \pm 0.002
DMS parameters					
DMSPt (nmol L^{-1})	25.9 \pm 1.9	59.6 \pm 0.7	44.6 \pm 1.3	8.0 \pm 0.4	15.1 \pm 0.5
DMS (nmol L^{-1})	1.1 \pm 0.02	0.7 \pm 0.02	2.1 \pm 0.2	1.1 \pm 0.02	1.3 \pm 0.1
DMSPt : Chl a ($\text{nmol } \mu\text{g}^{-1}$)	18.3 \pm 0.2	9.2 \pm 0.2	58.1 \pm 3.8	6.2 \pm 0.3	61.1 \pm 3.4
DMS : DMSPt	0.02 \pm 0.001	0.03 \pm 0.002	0.05 \pm 0.004	0.14 \pm 0.004	0.09 \pm 0.002

2.3 DMSP synthesis and production rates

De novo DMSP synthesis and gross production rates were determined for all bioassay experiments at each experimental time point, except for E01. The methods used are based on the approach of Stefels et al. (2009) and are described in detail in Archer et al. (2013). For each CO_2 level, triplicate rate measurements were determined. For each rate measurement 3×500 mL polycarbonate bottles were filled by gently siphoning water directly from each replicate bioassay bottle. Trace amounts of $\text{NaH}^{13}\text{CO}_3$, equivalent to $\sim 6\%$ of in situ dissolved inorganic carbon (DIC), were added to each 500 mL bottle. The bottles were incubated in the bioassay

incubation container with temperature and light levels as described above. Samples were taken at 0 h and then at two further time points over a 6–9 h period. At each time point, 250 mL was gravity-filtered in the dark through a 47 mm GF/F filter, the filter was gently folded and placed in a 20 mL serum vial with 10 mL of Milli-Q and one NaOH pellet, and the vial was crimp-sealed. Samples were stored at -20°C until analysis by proton transfer reaction mass spectrometer (PTR-MS) (Stefels et al., 2009).

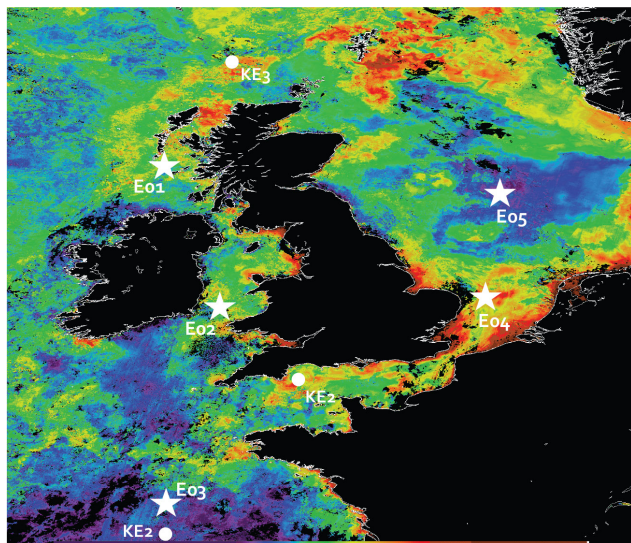


Figure 1. Locations of sampling in NW European shelf waters for bioassay experiments (white stars, E01–E05) and for kinetic experiments (white circles, KE1–KE3). Map shows Medium Resolution Imaging Spectrometer (MERIS) chlorophyll composite for period 6–12 June 2011 as a representative week of the sampling period (8 June–5 July 2011). Satellite image courtesy NERC Earth Observation Data Acquisition and Analysis Service (NEODAAS).

The specific growth rate of DMSP (μ DMSP) was calculated assuming exponential growth from

$$\mu_t = \alpha_k \times \text{AVG} \left[\left(\ln \frac{{}^{64}\text{MP}_{\text{eq}} - {}^{64}\text{MP}_{t-1}}{{}^{64}\text{MP}_{\text{eq}} - {}^{64}\text{MP}_t} \right) \right. \\ \left. \left(\ln \frac{{}^{64}\text{MP}_{\text{eq}} - {}^{64}\text{MP}_t}{{}^{64}\text{MP}_{\text{eq}} - {}^{64}\text{MP}_{t+1}} \right) \right], \quad (1)$$

(Stefels et al., 2009), where ${}^{64}\text{MP}_t$, ${}^{64}\text{MP}_{t-1}$ and ${}^{64}\text{MP}_{t+1}$ are the proportion of $1 \times {}^{13}\text{C}$ labelled DMSP relative to total DMSP at time t , at the preceding time point ($t-1$) and at the subsequent time point ($t+1$), respectively. Values of ${}^{64}\text{MP}$ were calculated from the protonated masses of DMS as follows: $\text{mass } 64 / (\text{mass } 63 + \text{mass } 64 + \text{mass } 65)$, determined by PTR-MS. ${}^{64}\text{MP}_{\text{eq}}$ is the theoretical equilibrium proportion of $1 \times {}^{13}\text{C}$ based on a binomial distribution and the proportion of tracer addition. An example of the change in proportion of mass ratio $64({}^{64}\text{MP})$ during incubations of water from experiment E05 at T48 for the different $p\text{CO}_2$ treatments is shown in Fig. S1 in the Supplement. An isotope fractionation factor α_k of 1.06 is included, based on laboratory culture experiments using *Emiliania huxleyi* (Stefels et al., 2009).

Gross DMSP production rates during the incubations ($\text{nmol L}^{-1} \text{h}^{-1}$) were calculated from μ DMSP and the initial particulate DMSP (DMSPp) concentration of the incubations. Concentrations of DMSPp were determined at each time point by gravity filtering 7 mL of sample onto a 25 mm GF/F filter and preserving the filter in 7 mL of 35 mM H_2SO_4

in Milli-Q water. DMSPp concentrations were subsequently measured as DMS following alkaline hydrolysis (see above).

2.4 Biological DMS consumption (BC) and estimation of gross DMS production (GP)

Gross DMS production (GP) by the whole microbial community and bacterial DMS consumption (BC), were determined by dark incubations of whole seawater with ${}^{13}\text{C}$ -DMS additions. Incubations were performed at each experimental time point of the five bioassay experiments. Six incubations were performed per experiment (i.e. three time points for both ambient and 750 μatm CO_2 treatments).

${}^{13}\text{C}$ -DMS solutions were prepared by reducing ${}^{13}\text{C}$ -dimethyl sulfoxide (DMSO) (100 μL 99 % DMSO, Sigma Aldrich Co., diluted in 900 μL Milli-Q) using sodium borohydride (NaBH_4 , 1 g left for 5 min). The reactants were purged (20 mL min^{-1} for 20 min) and ${}^{13}\text{C}$ -DMS collected in a 1/16" PTFE loop submerged in liquid nitrogen. The ${}^{13}\text{C}$ -DMS was rinsed into a 20 mL glass serum vial by syringing 15 mL of Milli-Q through the sample loop. The serum vial was crimp-sealed and stored in the dark at 4 °C. The primary solution underwent two serial dilutions in Milli-Q to produce a working solution.

For each incubation, 500 mL of seawater were siphoned from the bioassay bottle into an acid-washed (1 % HCl) and thoroughly rinsed 1 L Tedlar bag. Once filling was complete, any bubbles and headspace were gently expelled from the bag. Each bag was spiked with small volumes (100–150 μL) of a working solution of ${}^{13}\text{C}$ -DMS (in Milli-Q water) to give concentrations of 0.1–0.3 nM. After spiking, the bags were left for 1 h to allow complete homogenisation of the tracer. Bags were incubated in the dark, and concentrations of ${}^{13}\text{C}$ -DMS and ${}^{12}\text{C}$ -DMS were monitored to determine ${}^{13}\text{C}$ -DMS loss rates and net and gross DMS. Subsamples (20 mL) were withdrawn using a glass syringe at 0 h and at three further time points over a 10–12 h period. The samples were gently filtered through a Millipore filtration unit containing a 25 mm GF/F filter, directly into a 10 mL glass syringe, and 8 mL of filtered seawater were injected into a glass purge tower. The addition of air and bubbles was avoided or minimised at all times. The sample was purged for 8 min at 90 mL min^{-1} , dried with a PTFE counterflow Nafion drier and trapped in a 1/16" PTFE loop held in liquid nitrogen. Once purging was complete, the sample loop was rapidly submerged in boiling water, injecting the sample into an Agilent 5973° N gas chromatograph with a 60 m DB-VRX capillary column and mass spectral detector (MSD). The oven temperature was held at 60 °C for 8 min and was increased sharply to 220 °C for the remainder of the 10 min runtime. DMS and ${}^{13}\text{C}$ -DMS eluted from the column at ~ 5.3 min. The MSD was operated in single ion mode (SIM) and was programmed to detect the following ions: m/z 62, 61 and 47 for ${}^{12}\text{C}$ -DMS; m/z 64 for ${}^{13}\text{C}$ -DMS; and m/z 68 for deuterated DMS (CD_3SCD); of this, 100 μL of a 5 ppmv gas standard was injected into the

purge gas stream for every sample in order to monitor and correct for system sensitivity and drift. By taking the ratio of m/z 62 or 64 to m/z 68, a greatly improved precision of analysis was attained.

Calibrations were performed using pure DMS (>99 %, Sigma Aldrich Co.) diluted in Milli-Q water. A primary standard was gravimetrically prepared, and then serial dilutions were performed to obtain a working standard of 0.3 ng S mL^{-1} . Multi-point calibrations, from 0 to 3.5 ng S mL^{-1} , were performed every 3 days for the duration of the cruise. Detection limits for $^{12}\text{C-DMS}$ and $^{13}\text{C-DMS}$ were 0.1 ng S and 0.03 ng S , respectively. The lower detection limit for $^{13}\text{C-DMS}$ is the result of lower background concentrations of this isotope in blank measurements. Average analytical precision based on triplicate samples was $\sim 10\%$.

Rates of BC ($\text{nmol L}^{-1} \text{ d}^{-1}$) were estimated from the slope of the linear decrease in $^{13}\text{C-DMS}$ concentrations over the 10–12 h incubation period (see Fig. S2 in the Supplement). DMS loss via photochemistry and gas exchange was excluded, so the $^{13}\text{C-DMS}$ loss is considered to be equivalent to biological consumption. To scale to in situ DMS concentrations, BC rates were first divided by the concentration of $^{13}\text{C-DMS}$ tracer (giving first-order rate constants, d^{-1}) and multiplied by in situ DMS concentrations. The $^{12}\text{C-DMS}$ change during the incubations represents the net DMS production rate. The GP was estimated as the sum of net DMS production and BC.

Additions of $^{13}\text{C-DMS}$ ranged from 10 to 100 % of ambient DMS concentrations. Large relative additions of $^{13}\text{C-DMS}$ were unavoidable when ambient DMS concentrations were low ($< 1 \text{ nmol L}^{-1}$) due to the limits of detection of the method. The following equation was used to correct BC rates for any enhancement caused by tracer addition ($r\text{DMS}_t$), (Rees et al., 1999), which was originally described for the correction of ^{15}N ammonium uptake rates:

$$r\text{DMS}_t = \frac{r\text{DMS}_o}{\text{DMS}_{\text{tot}} / (K_s + \text{DMS}_{\text{tot}}) \cdot (K_s + \text{DMS}_a) / \text{DMS}_a}, \quad (2)$$

where $r\text{DMS}_t$ is the loss rate adjusted for stimulation by tracer ($\text{nmol L}^{-1} \text{ d}^{-1}$), $r\text{DMS}_o$ is the original loss rate ($\text{nmol L}^{-1} \text{ d}^{-1}$), DMS_{tot} is $[\text{DMS}]_{\text{ambient}} + [^{13}\text{C-DMS}]$ (nmol L^{-1}), DMS_a is $[\text{DMS}]_{\text{ambient}}$ (nmol L^{-1}), and K_s is the half-saturation parameter (nmol L^{-1}). The value of K_s was taken as the mean of the K_s determined through three kinetic experiments described in the section below. The applied corrections resulted in decreases in the biological DMS consumption rates of 8–51 %; the larger uncertainties are associated with relatively low in situ DMS concentrations, thus resulting in relatively high tracer additions. Applying the maximum (25.0 nmol L^{-1}) and minimum (4.5 nmol L^{-1}) K_s values to the correction gives the following uncertainties on the loss rates: E01 13.8–24.9 %, E02 23.1–39.7 %, E03 7.0–9.1 %, E04 9.7–12.7 % and E05 1.1–7.7 %. Using the standard error of mean K_s to the correction (shown in Table 2) results in uncertainty on loss rates of E01 3.8–6.9 %,

E02 6.3–9.5 %, E03 1.6–2.0 %, E04 1.9–2.3 % and E05 0.3–1.6 %.

2.5 Biological DMS consumption: kinetic parameters

Three additional experiments, hereafter referred to as KE1, KE2 and KE3, were conducted to determine BC kinetic parameters. As it was not logistically feasible to conduct the kinetic experiments in parallel to the bioassay incubations, the three sites were chosen to encompass contrasting NW European shelf waters. The locations of sampling for kinetic experiments are shown in Fig. 1. Unfiltered surface seawater (3–5 m) was siphoned into five 1 L Tedlar bags that had been acid-washed with 1 % HCl and thoroughly rinsed three times with ultrapure water. Once filling was complete, any bubbles and headspace were gently expelled from the bag. For each experiment, increasing concentrations of $^{13}\text{C-DMS}$ were added to each bag, ranging from at or below in situ concentrations up to 74 nmol L^{-1} . After the addition, the bags were left for 1 h to allow complete homogenisation of the tracer. The bags were incubated for up to 12 h in the dark at in situ seawater temperature, and samples were processed and analysed as described above.

Initial DMS concentrations showed a wide range, from 1.0 nmol L^{-1} in KE1 to 16.8 nmol L^{-1} in KE3 (see Table 2 and water column profiles in Fig. S3 in the Supplement). A large range of DMS : DMSPt ratios were also encountered, with a value of 0.2 for KE3, which was an order of magnitude higher than the values of 0.02 and 0.03 for KE1 and KE2.

A summary of the Michaelis–Menten kinetic parameters for the three experiments, obtained through non-linear regression using Minitab 16.0 statistical software, are given in Table 2. Kinetic curves (see example Fig. S4 in the Supplement) were based on five to six data points; replicate samples were unfeasible due to the time taken to analyse all samples at each of four time points over a $\sim 10 \text{ h}$ period. However, the non-linear regressions for each experiment were significant ($P < 0.05$). The kinetic parameters generated in this study represent the activity of natural assemblages rather than the activity of single enzymes or species and showed a similarly broad range to in situ DMS(P) characteristics. Half-saturation constants (K_s) ranged from 4.5 nmol L^{-1} in KE3 to 25.0 nmol L^{-1} in KE1, with KE2 displaying an intermediate K_s value of 11.4 nmol L^{-1} . Thus, an inverse relationship between in situ DMS concentrations and K_s was apparent. Maximum DMS consumption rates (V_{max}) were also variable. KE3 displayed the lowest V_{max} of only $1.3 \text{ nmol L}^{-1} \text{ d}^{-1}$, and this time KE2 gave the highest values with $25.9 \text{ nmol L}^{-1} \text{ d}^{-1}$. Despite having the highest K_s and lowest in situ DMS concentrations, KE1 yielded an intermediate V_{max} of $10.9 \text{ nmol L}^{-1} \text{ d}^{-1}$.

Table 2. Kinetic parameters (K_s (half-saturation constant), V_{\max} (maximum ^{13}C -DMS consumption rate)) and turnover time of DMS due to BC (τ_{BC}) for ^{13}C -DMS loss rates at three contrasting sites in NW European shelf waters. Kinetic parameters were calculated by fitting data to the Michaelis–Menten equation through non-linear regression of loss rate vs. ^{13}C -DMS concentration data from three kinetic experiments (See Fig. S4 in the Supplement). Initial in situ DMS concentrations measured at 0 h of each kinetic experiment are also shown.

Experiment	Date	Initial [DMS] (nmol L ⁻¹)	DMS : DMSPt (nmol L ⁻¹)	$K_s \pm \text{SE}$ (nmol L ⁻¹ d ⁻¹)	$V_{\max} \pm \text{SE}$	r^2 (d)	τ_{BC}
KE1	19 June 2011	1.0	0.02	25.0 ± 13.8	10.9 ± 2.5	0.91	0.09
KE2	24 June 2011	3.8	0.03	11.4 ± 6.7	25.9 ± 7.3	0.96	0.15
KE3	5 July 2011	16.8	0.2	4.5 ± 1.1	1.3 ± 0.1	0.89	12.9
Mean				13.6 ± 7.2	12.7 ± 3.3		

2.6 Total bacteria abundance

Samples for the determination of total bacteria abundance were taken in triplicate at the start of all incubations for BC and GP. Twenty μL of glutaraldehyde solution (Grade 1, 50 % in H_2O , Sigma Aldrich Co.) was added to 2 mL samples, and the vials were fixed for 30 min at 4 °C, followed by snap freezing in liquid nitrogen and storage at -80°C until analysis. Bacteria were counted by flow cytometry according to Marie et al. (1999). Briefly, thawed samples were diluted with Tris-EDTA buffer (10 mM Tris-HCl and 1 mM EDTA, pH 8) and stained with the green fluorescent nucleic acid-specific dye SYBR-Green I (Molecular Probes, Invitrogen Inc.) at a final concentration of 1×10^{-4} of the commercial stock in the dark at room temperature for 15 min. Bacteria were discriminated in bivariate scatter plots of green fluorescence versus side scatter.

2.7 Ancillary parameters

A description of methodologies for all ancillary parameters described in Table 1 (carbonate chemistry, nutrients, total and size-fractionated chlorophyll *a*) and for the enumeration of small phytoplankton by flow cytometry (Fig. 2) is given in Richier et al. (2014a).

3 Results

3.1 Experimental bioassays: starting conditions

The design of this study allowed an assessment of the response of surface ocean communities to high CO_2 during the most biologically productive time of year by sampling a variety of seasonally stratified (E01, E03, E05) and perennially mixed (E02, E04) sites, both on- and off-shelf (Fig. 1). Initial conditions generally displayed typical NW European shelf summertime characteristics, with low concentrations of nutrients ($< 1.1 \mu\text{M}$ total organic nitrogen (TON), $\sim 0.1 \mu\text{M}$ P) and a range of Chl *a* concentrations ($0.8\text{--}3.3 \mu\text{g L}^{-1}$) reflecting the heterogeneous spatial distribution of marine productivity in shelf sea waters. In situ $p\text{CO}_2$ concentrations

were similarly variable, ranging from 334 μatm for E02 to 401 μatm for E04 (See Table 1). Further detail is given elsewhere (Richier et al., 2014a).

3.2 DMSPt and DMS: concentrations and ratios

Triplicate bottles for each treatment displayed similar values and trends of DMSPt over the course of each experiment. Initial concentrations in the five bioassays spanned a wide range, from 8.0 nmol L⁻¹ for E04 to 59.6 nmol L⁻¹ for E01 (Table 1). There was a net increase in DMSPt for all ambient control incubations after 96 h, with the greatest increase seen over the first 48 h. For all experiments, a clear response to increasing levels of CO_2 was observed (Fig. 2a–e), with a large number of significant reductions in DMSPt with increasing CO_2 concentrations after 48 h (analysis of variance (ANOVA), Holm–Sidak, $P < 0.05$; Table S2 in the Supplement). After 96 h, concentrations showed some recovery in high- CO_2 treatments for E02 and E04, but the response persisted for E01, E03 and E05. In addition, when all data were included in a single analysis, a significant negative relationship between DMSPt and $[\text{H}^+]$ data was seen (ANOVA, significance of F -ratio $P < 0.001$; Table S3 in the Supplement).

Again, concentrations and trends of DMS from triplicate bottles within each treatment were similar for all experiments. Initial mean concentrations of DMS (Fig. 2f–j) varied by a factor of 3, from 0.7 nmol L⁻¹ (E02) to 2.1 nmol L⁻¹ (E03), and higher DMS concentrations tended to be associated with lower Chl *a* (Table 1). Net DMS accumulation was observed in all ambient control incubations over 96 h. There was a clear response to high CO_2 in all experiments, with significantly elevated DMS concentrations, predominantly after 48 h (ANOVA, Holm–Sidak, $P < 0.05$; Table S2 in the Supplement). The response became more variable by 96 h, with rapid rises in DMS in ambient controls for E01, E03 and E04 between 48 and 96 h, resulting in concentrations similar to those under high CO_2 . For all experiments at each time point (with the exception of E04 at 96 h) significant positive relationships between DMS concentrations and $[\text{H}^+]$ were observed (Table S3 in the Supplement). The relationship between these variables was strongest at 48 h ($r^2 = 0.58\text{--}0.92$,

$P < 0.01$) and generally weakened at 96 h ($r^2 = 0.35 - 0.79$, $P < 0.05$).

In summary, large increases in mean DMS concentrations relative to ambient controls were observed in all bioassays: 110 % (28–223 %) at 550 μatm , 153 % (56–295 %) at 750 μatm and 225 % (79–413 %) at 1000 μatm . By contrast, mean DMSPt concentrations showed a consistent decrease, but to a lesser extent than DMS: 28 % (18–40 %) at 550 μatm , 44 % (18–64 %) at 750 μatm and 52 % (24–72 %) at 1000 μatm .

Initial DMS : DMSPt ratios ranged from 0.02 for E01 to 0.14 for E04 (Fig. S5 in the Supplement). This ratio gradually increased over 96 h (except in E04) and for all experiments was significantly correlated with increasing $[\text{H}^+]$ after both 48 h and 96 h (Fig. 3 and Table S3 in the Supplement; ANOVA of regression, F ratio $P < 0.05$). DMS : Chl a ratios generally followed similar trends to DMS : DMSPt (Fig. S5 in the Supplement). Significant positive relationships between DMS : Chl a and $[\text{H}^+]$ were identified for all experiments at 48 h (ANOVA of regression, F ratio $P < 0.001$, except E04 $P < 0.05$; Table S3 in the Supplement). By 96 h, this relationship remained significant for all experiments but was negative for E01 and E04.

DMSPt : Chl a also showed large variation between experiments, from $< 30 \text{ nmol } \mu\text{g}^{-1}$ in E02 up to $\sim 150 \text{ nmol } \mu\text{g}^{-1}$ in E03 (Fig. S5 in the Supplement). In general, increasing $[\text{H}^+]$ was associated with a decrease in DMSPt : Chl a , but this relationship was found to be significant only for E01 and E04 at 48 h. By 96 h, the majority of experiments displayed a significant negative relationship between these variables (ANOVA of regression, F ratio $P < 0.01$; Table S3 in the Supplement).

3.3 Plankton community and OA response

In general, an increase in the abundance of small phytoplankton ($< 10 \mu\text{m}$, pico- and nanophytoplankton) was seen over the experimental period, indicating growth within the bioassay bottles (Fig. 2k–o). For E02–E05, abundances were significantly lower under high CO_2 at both 48 h and 96 h (ANOVA, Holm–Sidak, $P < 0.05$; Table S4 in the Supplement). By contrast, there were significant increases in abundance under high CO_2 (750 and 1000 μatm) at 96 h for E01 (ANOVA, Holm–Sidak, $P < 0.001$; Table S4 in the Supplement). The reader is directed to Richier et al. (2014a) for further description of the response of small phytoplankton.

3.4 DMSP synthesis and production

Initial DMSP synthesis rate constants (μDMSP) ranged from 0.33 d^{-1} in E05 to 0.96 d^{-1} in E03. Rate constants tended to decrease over the course of 96 h to $\sim 0.10 - 0.50 \text{ d}^{-1}$ (Fig. 4a–d). The effect of CO_2 treatment on μDMSP was variable. Marked and significant decreases in μDMSP at all high- CO_2 treatments relative to ambient controls were seen for E02 at

48 h and 96 h (analysis of covariance (ANCOVA), $P < 0.01$; Table S5 in the Supplement) and for E05 at 48 h (ANCOVA, $P < 0.01$; Table S5 in the Supplement). For E03 and E04, the response of μDMSP to high- CO_2 treatments was more variable, with a number of significant differences from ambient CO_2 identified (see Table S5 in the Supplement for results of ANCOVA), but of an inconsistent direction relative to ambient CO_2 .

Temporal trends in DMSP production rates corresponded closely with those for μDMSP (Fig. 4e–h). Initial DMSP production rates ranged from $7.1 \text{ nmol L}^{-1} \text{ d}^{-1}$ in E05 to $37.3 \text{ nmol L}^{-1} \text{ d}^{-1}$ in E03. For E02 and E05, clear decreases in DMSP production rates were observed in the high- CO_2 treatments. In E02, this difference was maintained for the duration of the experiment with a mean of $12.0 \text{ nmol L}^{-1} \text{ d}^{-1}$ at ambient CO_2 , compared to $1.8 - 3.1 \text{ nmol L}^{-1} \text{ d}^{-1}$ at elevated CO_2 . Similarly large decreases in mean DMSP production were seen in E05 ($2.9 - 11.1 \text{ nmol L}^{-1} \text{ d}^{-1}$ high CO_2 , $13.4 \text{ nmol L}^{-1} \text{ d}^{-1}$ ambient CO_2). Similarly to μDMSP , the response to high CO_2 was more variable for E03 and E04.

3.5 Bacterially mediated DMS processes

3.5.1 Total bacteria abundance

Initial abundances of bacteria (Fig. 5a–e) in the sub-incubations for BC and GP rates were statistically similar (Kruskal–Wallis $H = 3.273$, $df = 3$, $P = 0.415$), ranging from $0.83 (\pm 0.01)$ to $1.00 (\pm 0.16) \times 10^6 \text{ cells mL}^{-1}$ (no data available for E01 0 h). For E01, E02, E04 and E05 bacterial abundance increased with increasing CO_2 . Small differences in abundance at 48 h were followed by large increases in bacteria at 750 μatm by 96 h. By contrast, a decrease in bacterial abundance in response to increased CO_2 was observed for E03.

3.5.2 Biological DMS consumption (BC)

Rates of biological DMS consumption (BC) across the five bioassay experiments ranged from 0.2 ± 0.1 to $8.6 \pm 1.6 \text{ nmol L}^{-1} \text{ d}^{-1}$, with the highest overall mean values observed during E01 at Mingulay Reef ($3.6 \pm 0.7 \text{ nmol L}^{-1} \text{ d}^{-1}$) and the lowest during E02 in the Irish Sea ($0.5 \text{ nmol L}^{-1} \text{ d}^{-1}$) (see Fig. 5f–j and Table S6 in the Supplement). All rates fell well within the range of a variety of previous studies ($0.02 - 8.8 \text{ nmol L}^{-1} \text{ d}^{-1}$; Bailey et al., 2008, Kiene et al., 2007, Toole and Siegel 2004, Toole et al., 2006, del Valle et al., 2009, Vila-Costa et al., 2008, Zubkov et al., 2002, 2004). Overall, no consistent response of BC to CO_2 treatment was observed. For E01 and E02, BC was greater at high CO_2 , with significant differences after 48 h (ANOVA F ratio $P < 0.05$). For E03, BC was lower under high CO_2 , although the differences were not significant. For E04 and E05, significant decreases in BC after 96 h were observed (ANOVA F ratio $P < 0.05$).

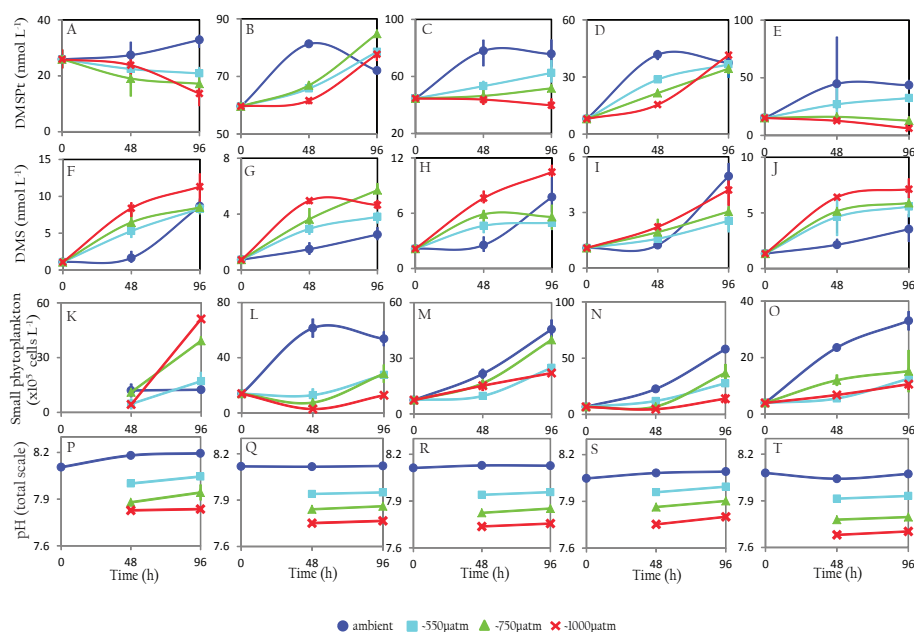


Figure 2. Concentrations (nmol L^{-1}) of total DMSP (a–e) and DMS (f–j) during five bioassay experiments; abundance of total small phytoplankton ($<10 \mu\text{m}$) (k–o) ($\times 10^5 \text{ cells L}^{-1}$) and pH (total scale) (p–t). See Table 1 for specific $p\text{CO}_2$ and pH for each experiment. Different scales are used on plots to ensure trends are visible. Values shown are means of experimental triplicates, and error bars indicate the standard error (SE). For pH measurements, SE generally fell within the bounds of the symbols used on the plots. Smoothed lines on plots do not represent extrapolation of data between time point measurements but are used to highlight trends.

3.5.3 Biological DMS turnover

DMS turnover time due to biological consumption (τ_{BCD}), calculated as the inverse of the loss rate constant (k_{BC} , d^{-1}) (Fig. 5k–o and Table S6 in the Supplement), ranged from <1 d (E01, E05) to a maximum of 12.3 d (E02). Similarly to BC, there was a lack of consistent response to high CO_2 . For experiments E03–E05, turnover over times were consistently higher at high CO_2 , but the differences were only significant for E03 (48 h) and E04 (96 h).

3.5.4 Gross DMS production (GP)

Mean gross production rates of DMS (GP) in the five bioassay experiments ranged from undetectable levels during E02 up to a maximum of $8.7 \pm 1.4 \text{ nmol L}^{-1} \text{ d}^{-1}$ during E05 (Fig. 5p–t, Table S6 in the Supplement). The negative value observed at 48 h in the ambient treatment for E02 was not significantly different from 0, so GP was considered to be undetectable in this case. Overall, a response of GP to high CO_2 was variable or undetectable. GP was significantly elevated at high CO_2 for E02 at 96 h and E03 after 48 h, whilst a significant decrease in GP was observed for E04 at 96 h (ANOVA F ratio $P < 0.05$). No significant differences were seen for E01, E04 and E05.

4 Discussion

Despite variability in physical, biological and biogeochemical characteristics of sampling stations, experimental bioassays gave highly consistent DMS(P) responses to OA, affirming the strength of the experimental approach adopted here. Large increases in mean DMS concentrations relative to ambient CO_2 controls were observed in all bioassays: 110 % (28–223 %) at 550 μatm , 153 % (56–295 %) at 750 μatm and 225 % (79–413 %) at 1000 μatm . By contrast, mean DMSP concentrations showed a consistent decrease: 28 % (18–40 %) at 550 μatm , 44 % (18–64 %) at 750 μatm and 52 % (24–72 %) at 1000 μatm . Our results are in opposition to the majority of results from mesocosm studies. We examine the possible drivers of the observed responses in the following section.

4.1 Influence of plankton community response on DMS(P)

Primarily as a result of the characteristic community dynamics of mesocosm experiments, our current knowledge of the algal physiological effects of OA on the production of DMSP and DMS is minimal. During a mesocosm experiment in Arctic waters, increasing CO_2 resulted in elevated gross primary productivity, partly accounted for by an increase in net production of the autotrophic dinoflagellate *Heterocapsa rotundata* (Archer et al., 2013). The net increase in *H. rotundata*

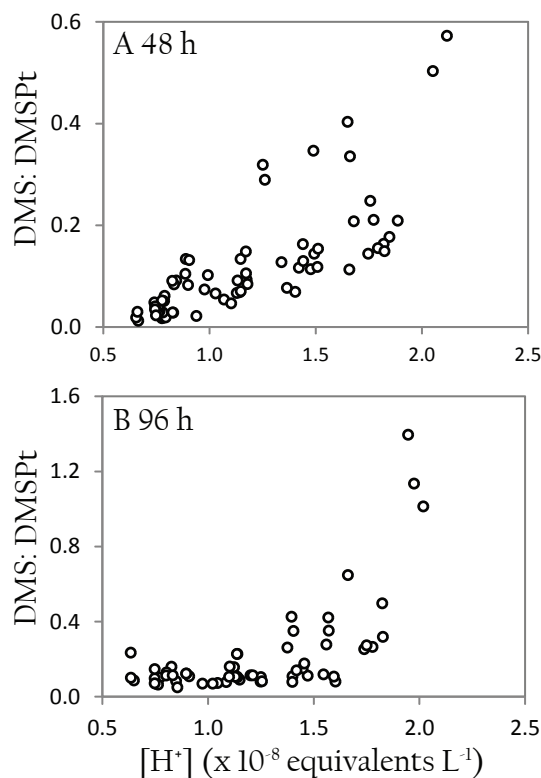


Figure 3. Relationship between DMS : DMSPt and H^+ concentration, ($[H^+] \times 10^{-8}$ equivalents L^{-1}) at 48 h (a) and 96 h (b) for all data from all five bioassay experiments.

was evident as an increase in DMSP production rates and concentrations at high CO_2 . Despite observations of a stimulating effect of CO_2 on photosynthesis and carbon fixation in a range of other phytoplankton taxa and natural assemblages (Riebesell and Tortell, 2011), there was no evidence for enhanced productivity during the bioassay experiments. Indeed, primary production appeared to decrease with increasing $[H^+]$. ^{14}C -based measurements of primary production for E02 and E03 showed a tendency to decrease under high CO_2 (A. Poulton, personal communication, 2013), whilst in E03, E04 and E05 significantly lower [Chl *a*] with increasing CO_2 was also observed (see Richier et al., 2014a).

Over the shorter timescale of the present study, changes in phytoplankton composition were not expected to influence the DMS(P) response to the same extent as seen in mesocosm experiments. However, it is apparent in the abundance of small phytoplankton (Fig. 2k–o), and is elaborated on by Richier et al. (2014a), that phytoplankton composition altered rapidly between treatments in the majority of the experiments. In all experiments, except E01, the abundance of small phytoplankton ($< 10 \mu m$) was significantly lower under high CO_2 (Fig. 2k–o, Table S4). Furthermore, specific rates of DMSP synthesis ($\mu DMSP$) and DMSP production rates were either insensitive to high CO_2 (E03, E04) or showed marked declines (E02, E05) (Fig. 4a–d). As small

phytoplankton can contribute between 40 % and 57 % to the total DMSP pool (Archer et al., 2011), it is likely that decreases in DMSPt were primarily driven by the observed decreases in abundance of this group, accompanied in some cases (E02, E05) by the influence of a decrease in DMSP synthesis.

This general decrease in growth of small phytoplankton also coincided with significant increases in DMS : DMSPt, suggesting a relationship between these two responses. OA results in a reduction in buffer capacity that may affect proton concentration ($[H^+]$) and/or regulation at the cell membrane surface of phytoplankton. Larger cells ($> 25 \mu m$) possess thicker boundary layers and under present-day conditions may experience such changes over the course of a diel cycle (Flynn et al., 2012). As such, they may be better adapted than smaller cells ($< 25 \mu m$) to the higher $[H^+]$ that may be encountered under future OA. During the experimental bioassays, rapid changes to seawater chemistry may have induced changes to external cell surface $[H^+]$ beyond those experienced by small cells in the present-day oceans, resulting in deleterious effects on the growth of this fraction of the population. This may explain the reduced growth of small phytoplankton ($< 10 \mu m$) under high CO_2 in most experiments, summarised here in Fig. 2 (k–o and Table S4 in the Supplement) and discussed further by Richier et al. (2014a). This response may be compared to those observed when phytoplankton communities are subjected to other stressors. Gali et al. (2013) proposed that exposure to sublethal or lethal levels of ultraviolet radiation (UVR) could induce an increase in cell membrane permeability, eventually triggering apoptosis. This would lead to the release of intracellular DMSP, increasing its availability for catabolism by bacteria and/or extracellular DLA (DMSP lyase activity). In the bioassays, DMSPt concentrations fell and DMS production was stimulated, suggesting that the induced changes to carbonate chemistry may have resulted in an increase in cell permeability and lysis (Flynn et al., 2012; Richier et al., 2014a), leading to increased DMS release from cells. As discussed above, small phytoplankton can contribute a large proportion to the total DMSP pool, and so possess a large potential for DMS production (Archer et al., 2011). Thus, sublethal/lethal cellular damage to this fraction of the community induced by rising $[H^+]$ may have resulted in the strong increase in DMS concentrations.

The same response was seen in E01 despite an increase in abundance of small phytoplankton cells with increasing CO_2 (Fig. 2k). Uniquely, E01 at Mingulay Reef was dominated by cryptophytes ($\sim 10 \mu m$), whereas all others comprised a mainly $< 10 \mu m$ -sized community. Despite a similar overall response in DMS standing stocks, differences in initial community structure could result in a different physiological response to increased CO_2 . Rather than cells releasing DMSP/DMS as described above, a physiologically mediated overflow mechanism may have played a role. The cellular release of DMS is thought to facilitate the removal of surplus

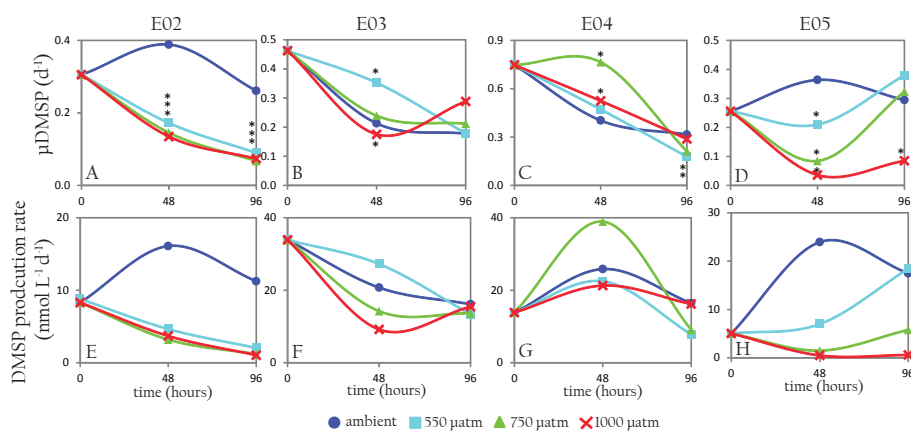


Figure 4. De novo synthesis of DMSP ($\mu\text{DMSP}, \text{d}^{-1}$) (a–d) and DMSP production rates ($\text{nmol L}^{-1} \text{d}^{-1}$) (e–h) for E02–E05 (data not available for E01). Asterisks (*) denote significant differences from ambient CO_2 bioassays (significance of F ratio from ANCOVA, $p < 0.05$). Smoothed lines on plots do not represent extrapolation of data between time point measurements but are used to highlight trends.

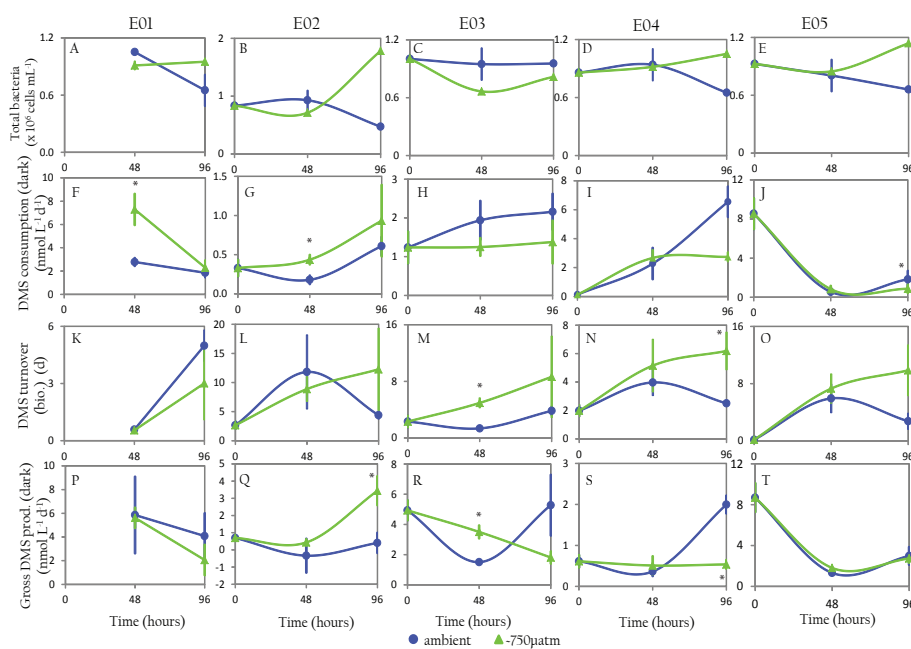


Figure 5. DMS consumption rates ($\text{nmol L}^{-1} \text{d}^{-1}$) (a–e), biological DMS turnover (d) (f–j), DMS gross production rates (k–o) and total bacteria counts (cells mL^{-1}) (p–t) during five bioassay experiments at ambient $p\text{CO}_2$ and $\sim 750 \mu\text{atm}$. DMS turnover times (d) = $1 / \text{loss rate constant}$ ($k_{\text{BC}}, \text{d}^{-1}$). Data are summarised in Table S6 in the Supplement. Error bars indicate standard error on triplicate rate measurements. Asterisks (*) denote significant difference from ambient CO_2 bioassays (significance of F ratio from ANOVA, $p < 0.05$). No measurements were made at 0 h for E01. Smoothed lines on plots do not represent extrapolation of data between time point measurements but are used to highlight trends.

sulfur, carbon and energy, allowing the cell to continue functioning during periods of cellular stress or unbalanced growth (Stefels, 2000). This process depends on a direct up-regulation of the conversion of DMSP to DMS via DLA. Previous studies have demonstrated an increase of up to an order of magnitude in DMS production in phytoplankton exposed to UV stress (Sunda et al., 2002; Archer et al., 2010; Gali et al., 2013). The observed increases of DMS : DMSPt with

increasing CO_2 suggest that elevated $[\text{H}^+]$ may drive an analogous response, stimulating increases in turnover of DMSP to DMS. This could be driven by the apparent susceptibility of smaller phytoplankton cells to changes in $[\text{H}^+]$ (Flynn et al., 2012; Richier et al., 2014a). Such a process could, to some extent, be relevant to the results of all bioassay experiments.

4.2 Influence of bacterial community response on DMS(P)

Previous OA studies suggest that increased primary production and photosynthesis at high CO₂ may stimulate bacterial production by increasing the availability of organic substrates for bacterial utilisation (Weinbauer et al., 2011; Engel et al., 2013; Piontek et al., 2013). Such conditions could generate a greater bacterial demand for DMSP sulfur, leading to an increase in bacterial DMSP catabolism via the de/de pathway and to reductions in gross DMS production (Kiene et al., 2000). This mechanism could explain some of the reduction in DMS concentrations under high CO₂ seen during mesocosm studies (Hopkins et al., 2010; Avgoustidi et al., 2012; Archer et al., 2013). These previous findings suggest that increased CO₂ may stimulate bacterial production and (i) increase bacterial DMSP demethylation/demethiolation (de/de) and/or (ii) increase bacterial DMS consumption resulting in reduced gross DMS production.

However, there were few instances of significantly elevated dark DMS gross production rates in response to high CO₂ (Fig. 5 and Table S6 in the Supplement). For some experiments (E02, E03 and E04), trends in GP rates were comparable to temporal trends in net concentrations from the bioassays suggesting microbial DMS production is an important contributor to total DMS production, particularly in the latter stages of the bioassays (>48 h). However, it seems unlikely that the rapid increases in DMS yield seen in the first 48 h can be fully explained by an increase in bacterial DMS production or a reduction in consumption rates. The observed increase in DMS in the bioassays could imply a CO₂ effect resulting in a decrease in the activity of the de/de pathway, making more DMSP available for bacterial cleavage to DMS.

We also examined the response of biological consumption (BC) of DMS to elevated CO₂, a process thought to account for 50–80 % of total DMS loss in the surface oceans (Gabric et al., 1999; Simó, 2004). Increased bacterial production at high CO₂ may lead to increased bacterial consumption of DMS, resulting in a decrease in net DMS production. Rates of BC during this study ranged from 0.2 to 8.6 nmol L⁻¹ d⁻¹ falling well within the range of previous studies (0.02–8.8 nmol L⁻¹ d⁻¹; Bailey et al., 2008; Kiene et al., 2007; Toole et al., 2004, 2006; del Valle et al., 2009; Vila-Costa et al., 2008; Zubkov et al., 2002, 2004). Similarly, turnover times ranged from 0.2 to 12.3 d, again similar to earlier studies (0.7–18.7 d). The wide range in rates seen here reflects the highly heterogeneous spatial variability of both biomass and surface seawater DMS in NW European shelf waters during summertime.

In addition, the results from three kinetic experiments revealed a large range in values of K_s and V_{max} in the study waters implying contrasting levels of control of BC on surface ocean DMS concentrations in the study region (Table S6 in the Supplement). A broad range in these parameters is unsurprising given that the measured rates represent the activ-

ity of natural assemblages that will vary greatly in space and time in the dynamic shelf sea environment, rather than the activity of specific single enzymes or species. The three sites (KE1, KE2 and KE3) also encompassed a wide range of surface DMS concentrations of 1.0, 3.8 and 16.8 nmol L⁻¹, respectively, and this was likely a reflection of the contrasting BC characteristics of the sites (Fig. S3 in the Supplement). V_{max} ranged from 1.3 to 25.9 nmol L⁻¹ d⁻¹. K_s was inversely proportional to in situ DMS, demonstrating the saturation of BC at higher concentrations. For KE3, BC appeared to be close to saturation, suggesting a slow response of DMS consumers to rapidly increasing DMS concentrations at this site, reflected in low K_s of 4.5 nmol L⁻¹ and a long turnover time of ~13 d (Table S6 in the Supplement). Such large accumulations of DMS concentrations occur during the breakdown of phytoplankton blooms dominated by DMSP producers and have previously been attributed to low saturation kinetics of DMS consumers (Wolfe et al., 1999; Simó et al., 2000). Where DMS concentrations were lower for KE1 and KE2, K_s attained greater values of 11–25 nmol L⁻¹, and rapid turnover times of ~0.1 d were observed. Clearly, at these sites DMS consumers were able to exert a strong control over the accumulation of seawater DMS.

It is important to reiterate that it was not feasible to perform the kinetic experiments in parallel to the bioassay incubations for rates of BC. Therefore, the three sites chosen for kinetic experiments are assumed to give a good representation of the consumption kinetics likely to be encountered around NW European seas and, of course, within the bioassay experiments, with the recognised caveat that they do not precisely represent the in situ kinetics for each bioassay experiment. The uncertainties associated with the use of mean K_s determined from the three kinetic experiments and used to correct BC rates for tracer additions are given in the methodology section. However, given the broad range of consumption kinetics observed and the large range in situ DMS concentrations for each kinetic experiment (Table 2), it seems feasible that our kinetic experiments give a reasonable representation of the consumption kinetics within the bioassay incubations.

In the context of the bioassays, DMS concentrations generally did not exceed 9 nmol L⁻¹, apart from in two cases where concentrations of >10 nmol L⁻¹ were measured at 1000 μ atm in E01 and E03 (Fig. 2f and h). With K_s in the range of 4.5–25.0 nmol L⁻¹, it was unlikely that this process was saturated during the bioassays, allowing consumption to continue unabated despite rapid rises in DMS concentrations. In the two cases where DMS did exceed 10 nmol L⁻¹, it is possible that consumption kinetics reached saturation. However this was likely a result of, rather than cause of, the DMS CO₂ response. With this in mind, were the observed increases in DMS concentrations driven by CO₂-driven reductions in BC? Although variations in BC between ambient and 750 μ atm were observed (Fig. 5f–j, Table S6 in the Supplement), the observed differences were not consistent

enough to explain the changes in bulk DMS concentrations. Thus bacterial consumption of DMS in the bioassays did not appear to be sensitive to increasing CO₂ concentrations.

4.3 Exploring the regional variability

Despite this study targeting sites with a range of physical, biological and biogeochemical characteristics, the overall response to high CO₂ was remarkably consistent, suggesting limited regional variability. In Fig. 6, DMSPt and DMS concentrations under high CO₂ are normalised to those in ambient controls to allow comparison of the relative changes seen for each experiment. The general response is clear; however analysis of variance reveals some significant differences in the extent of the response at each station, suggesting varying levels of resilience in the communities.

The relative decreases in DMSPt concentrations were broadly consistent, ranging from 10 to 30 % relative to controls – except for E05 with a mean decrease of ~50 % (Fig. 6a). However, the relative increases in DMS were more variable between stations, from only ~10 % for E04 up to ~190 % for E01 (though accompanied by the greatest range) (Fig. 6b). Such variability is not surprising given the complex nature of DMSP and DMS seawater dynamics. Furthermore, the extent of the response to high CO₂ may be a reflection of the potential community DMS yield. Is it possible to attribute this variability to differences in the characteristics of each station given the available information?

Differences in phytoplankton abundance, speciation and size structure are likely to exert an influence on DMS yields. Initial Chl *a* concentrations were up to 12 times higher at E01 and E02 compared to E03–E05 (see Table 1), accompanied by clear differences in community size structure. E03–E05 were strongly dominated by the < 10 μm size class (29 724–155 764 cells mL⁻¹, compared to 5795 cells mL⁻¹ for E02 – no data for E01). By contrast, E01 and E02 saw a greater dominance by the > 10 μm size fraction (90–268.4 cells mL⁻¹, compared to 37.4–83.2 cells mL⁻¹ for E03–E05) (Richier et al., 2014a). The results of the ANOVA shown in Fig. 6 show that the sites also fall within these groupings based on the relative DMS response to high CO₂. As discussed in the previous section, size-related differences in community structure (< 10 μm E03–E05 vs. > 10 μm E01–E02) and differing responses/resiliencies of phytoplankton species are likely to contribute to differences in sensitivity to increasing CO₂ between the stations.

Further insight may be gained by considering the influence of microbial community processes on the observed differences between the stations. We observed differences in gross DMS production rates (dark) between stratified (E01, E03, E05) and mixed (E02, E04) stations. Measurements made at 0 h are most representative of in situ rates, and showed low levels of GP of 0.1–0.7 nmol L⁻¹ d⁻¹ at the mixed sites (E02 and E04) but relatively high rates of 4.9 and 8.7 nmol L⁻¹ d⁻¹ at E03 and E05 (no data for E01) (see

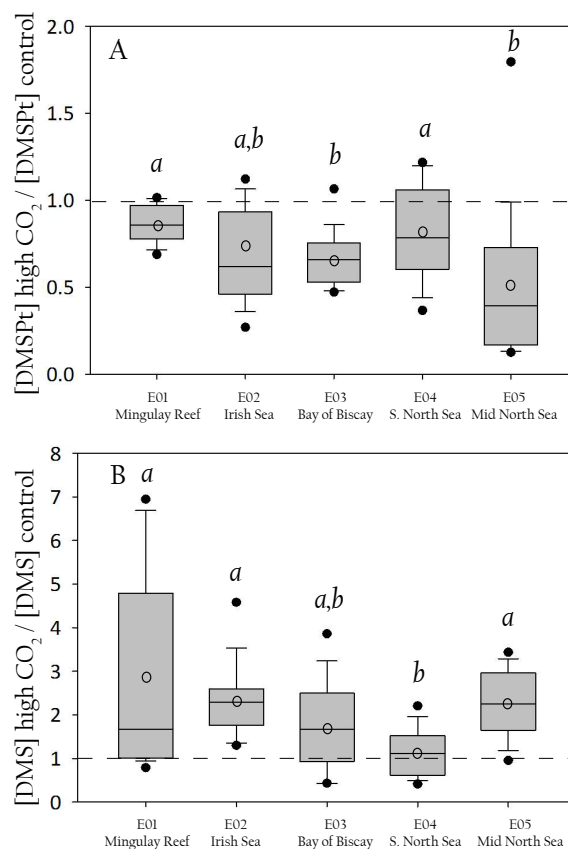


Figure 6. Box plots summarising relative differences ($[x]$ high CO₂ / $[x]$ control) in (a) DMSPt and (b) DMS between ambient control and high-CO₂ treatments for each experimental bioassay (all data from all time points). Plots show interquartile range (box), median values (horizontal line in box), mean values (open circles), range of data (error bars) and outliers (closed circles, outside $1.5 \times$ interquartile range). Italicised letters (*a*, *b*) indicate statistical groupings derived from one-way ANOVA and pairwise comparisons (Tukey's/Dunn's, significant differences between pairs if $P < 0.05$). Grey dashed line indicates a value of 1, i.e. no difference between ambient controls and high-CO₂ treatments.

Fig. 5 and Table S6 in the Supplement). This may indicate that the communities of stratified sites have a greater potential DMS yield, perhaps due to an increased importance of bacterial cleavage of DMSP to DMS in stratified waters, compared to a dominance of bacterial catabolism via the de/de pathway at the mixed sites. This may, for example, explain the large difference in relative DMS response between E01 and E04, despite a similar relative decrease in DMSPt (Fig. 6).

However, the above explanations are not sufficient to explain all of the variation in relative DMS response to high CO₂ that was observed across the five stations, as a range of interacting factors are likely to be involved. Further investigation is now needed to verify the extent of the influence of phytoplankton community structure and bacterial processes

on the sensitivity of surface ocean DMS systems to elevated CO₂ and to ascertain how the physical and biogeochemical characteristics of different regions may determine this response.

5 Summary and conclusions

We observed that rapid and short-term experimental manipulations of CO₂ and [H⁺] induced consistent, marked increases in DMS and decreases in DMSP, in contrast to results from mesocosm experiments. Mesocosms focus on longer timescales (up to 5 weeks) within the framework of a nutrient-induced phytoplankton bloom. This allows a “winners and losers” dynamic, encouraging shifts to species with greater resilience for change. The resultant DMS(P) response reflects the ensuing taxonomic changes (Vogt et al., 2008; Hopkins et al., 2010; Avgoustidi et al., 2012; Archer et al., 2013). The bioassay results we present represent an “acclimatory” response characterised by the lack of ability of small phytoplankton (<10 μm) to adapt to the altered carbonate chemistry. Our data are suggestive of an increase in stress-induced algal processes (increased cell permeability resulting in increased DMSP release and cleavage to DMS and/or direct up-regulation of intracellular DLA and DMS release) induced by the rapid changes to carbonate chemistry. However, this cannot be validated without direct measurements, so future studies could include better determination of algal-related processes, including measurements of dissolved DMSP concentrations to give an indication of loss of DMSP from phytoplankton cells and direct measurements of DLA (Steinke et al., 2000). In addition, more extensive tracer approaches may be useful to disentangle the fate of DMSP, particularly the balance between DMSP synthesis and breakdown or release by the algae. Finally, the influence of OA effects on grazing and subsequent DMSP cycling was not determined during this study and may warrant further investigation.

Although it would be inappropriate to extrapolate our small-scale, short-term results to future DMS sea-to-air fluxes, our study provides further evidence that the DMS system has a capacity to change in the face of future environmental change. Only one modelling study has attempted to quantify the climate response to OA-induced changes to sea surface DMS concentrations (Six et al., 2013). Though an important step forward, the study used model parameterisations based on empirical relationships between DMS and [H⁺] from mesocosm studies and is thus limited by the low level of understanding of the processes behind the observed responses to OA. The variables and rates we report improve our understanding of the sensitivity of the reduced sulfur cycle to future OA and may contribute to the development of a mechanistic approach to modelling future DMS concentrations (Polimene et al., 2012).

The Supplement related to this article is available online at doi:10.5194/bg-11-4925-2014-supplement.

Acknowledgements. This work is a contribution to the UK Ocean Acidification Research Programme (UKOA) which was jointly funded by the Department for Environment, Food and Rural Affairs (Defra), the Natural Environment Research Council (NERC) and the Department for Energy and Climate Change (DECC) under grant agreement no. NE/H017259/1. We are grateful to all members of the scientific party for aiding the success of cruise D366. In particular, we thank Toby Tyrell as lead PI of the UKOA Sea Surface Consortium, Eric Achterberg for leadership as chief scientist, and Sophie Richier and Mark Moore for the design and management of the experimental bioassays. Thanks also to Ross Holland for flow cytometry data, Alex Poulton for primary production data, Michelle Barnett for microscopy counts, Mark Stinchcombe for nutrient data and Cynthia Dumousseaud for carbonate chemistry measurements. Finally, we thank the captain and the crew of the *RRS Discovery* and the technical staff of the National Marine Facilities for support and assistance during the cruise. We are grateful to Tom Bell and two anonymous referees for comments that helped to significantly improve the manuscript.

Edited by: T. Tyrrell

References

- Andreae, M. O.: Ocean-atmosphere interactions in the global biogeochemical sulfur cycle, *Mar. Chem.*, 30, 1–29, 1990.
- Archer, S. D., Ragni, M., Webster, R., Airs, R. L., and Geider, R. J.: Dimethyl sulfoniopropionate and dimethyl sulfide production in response to photoinhibition in *Emiliana huxleyi*, *Limnol. Oceanogr.*, 55, 1579–1589, 2010.
- Archer, S. D., Tarran, G. A., Stephens, J. A., Butcher, L. J., and Kimmance, S. A.: Combining cell sorting with gas chromatography to determine phytoplankton group-specific intracellular dimethylsulphoniopropionate, *Aquat. Microb. Ecol.*, 62, 109–121, 2011.
- Archer, S. D., Kimmance, S. A., Stephens, J. A., Hopkins, F. E., Bellerby, R. G. J., Schulz, K. G., Piontek, J., and Engel, A.: Contrasting responses of DMS and DMSP to ocean acidification in Arctic waters, *Biogeosciences*, 10, 1893–1908, doi:10.5194/bg-10-1893-2013, 2013.
- Arnold, H. E., Kerrison, P., and Steinke, M.: Interacting effects of ocean acidification and warming on growth and DMS-production in the haptophyte coccolithophore *Emiliana huxleyi*, *Glob. Change Bio.*, doi:10.1111/gcb.12105, 2013.
- Avgoustidi, V., Nightingale, P. D., Joint, I., Steinke, M., Turner, S. M., Hopkins, F. E., and Liss, P. S.: Decreased marine dimethyl sulfide production under elevated CO₂ levels in mesocosm and in vitro studies, *Environ. Chem.*, 9, 399–404, 2012.
- Bailey, K. E., Toole, D., Blomquist, B., Najjar, R. G., Huebert, B., Kieber, D. J., Kiene, R. P., Matrai, P., Westby, G. R., and del Valle, D. A.: Dimethylsulfide production in Sargasso Sea eddies, *Deep-Sea Res. II*, 55, 1491–1504, 2008.

- Barnes, I., Hjorth, J., and Mihalopoulos, N.: Dimethyl sulfide and dimethyl sulfoxide and their oxidation in the atmosphere, *Chem. Rev.*, 106, 940–975, 2006.
- Brussaard, C. P. D., Noordeloos, A. A. M., Witte, H., Collenteur, M. C. J., Schulz, K., Ludwig, A., and Riebesell, U.: Arctic microbial community dynamics influenced by elevated CO₂ levels, *Biogeosciences*, 10, 719–731, doi:10.5194/bg-10-719-2013, 2013.
- Caldeira, K. and Wickett, M. E.: Anthropogenic carbon and ocean pH, *Nature*, 425, 365, 2003.
- Caldeira, K. and Wickett, M. E.: Ocean model predictions of chemistry changes from carbon dioxide emissions to the atmosphere and ocean, *J. Geophys. Res.*, 110, C09S04, doi:10.1029/2004JC002671, 2005.
- Charlson, R. J., Lovelock, J. E., Andreae, M. O., and Warren, S. G.: Oceanic phytoplankton, atmospheric sulphur, cloud albedo and climate, *Nature*, 326, 655–661, 1987.
- del Valle, D. A., Kieber, D. J., Toole, D. A., Brinkley, J., and Kiene, R. P.: Biological consumption of dimethylsulphide (DMS) and its importance in DMS dynamics in the Ross Sea, Antarctica, *Limnol. Oceanogr.*, 54, 785–798, 2009.
- Engel, A., Schulz, K. G., Riebesell, U., Bellerby, R., Delille, B., and Schartau, M.: Effects of CO₂ on particle size distribution and phytoplankton abundance during a mesocosm bloom experiment (PeECE II), *Biogeosciences*, 5, 509–521, doi:10.5194/bg-5-509-2008, 2008.
- Engel, A., Borchard, C., Piontek, J., Schulz, K. G., Riebesell, U., and Bellerby, R.: CO₂ increases ¹⁴C primary production in an Arctic plankton community, *Biogeosciences*, 10, 1291–1308, doi:10.5194/bg-10-1291-2013, 2013.
- Flynn, K. J., Blackford, J. C., Baird, M. E., Raven, J. A., Clark, D. R., Beardall, J., Brownlee, C., Fabian, H., and Wheeler, G. L.: Changes in pH at the exterior surface of plankton with ocean acidification, *Nature Clim. Change*, 2, 510–513, 2012.
- Gabric, A. J., Matrai, P. A., and Vernet, M.: Modelling the production and cycling of dimethylsulphide during the vernal bloom in the Barents Sea, *Tellus*, 51B, 919–937, 1999.
- Galí, M., Ruiz-González, Lefort, T., Gasol, J. M., Cardelús, C., Romera-Castillo, C., and Simó, R.: Spectral irradiance dependence of sunlight effects on plankton dimethylsulphide production, *Limnol. Oceanogr.*, 58, 489–504, 2013.
- Hendriks, I. E., Duarte, C. M., and Álvarez, M.: Vulnerability of marine biodiversity to ocean acidification: A meta-analysis, *Estuar. Coast. Shelf Sci.*, 86, 157–164, 2010.
- Hönisch, B., Ridgwell, A., Schmidt, D. N., Thomas, E., Gibbs, S. J., Sluijs, A., Zeebe, R., Kump, L., Martindale, R. C., Greene, S. E., Kiessling, W., Ries, J., Zachos, J. C., Royer, D. L., Barker, S., Marchitto, T. M., Moyer, R., Pelejero, C., Ziveri, P., Foster, G. L., Williams, B.: The geological record of ocean acidification, *Science*, 335, 1058–1063, 2012.
- Hopkins, F. E., Turner, S. M., Nightingale, P. D., Steinke, M., and Liss, P. S.: Ocean acidification and marine biogenic trace gas production, *P. Natl. Acad. Sci. USA*, 107, 760–765, 2010.
- Kiene, R. P., Linn, L. J., and Bruton, J. A.: New and important roles for DMSP in marine microbial communities, *J. Sea Res.*, 43, 209–224, 2000.
- Kiene, R. P., Kieber, D. J., Slezak, D., Toole, D. A., del Valle, D. A., Bisgrove, J., Brinkley, J., and Rellinger, A.: Distribution and cycling of dimethylsulphide, dimethylsulfoniopropionate, and dimethylsulfoxide during spring and early summer in the Southern Ocean south of New Zealand, *Aquat. Sci.*, 69, 305–319, 2007.
- Kiene, R. P. and Slezak, D.: Low dissolved DMSP concentrations in seawater revealed by small-volume gravity filtration and dialysis sampling, *Limnol. Oceanogr. Meth.*, 4, 80–95, 2006.
- Kim, J.-M., Lee, K., Yang, E. J., Shin, K., Noh, J. H., Park, K.-T., Hyun, B., Jeong, H.-J., Kim, J.-H., Kim, K. Y., Kim, M., Kim, H.-C., Jang, P.-G., and Jang, M.-C.: Enhanced production of oceanic dimethylsulphide resulting from CO₂-induced grazing activity in a high CO₂ world, *Environ. Sci. Technol.*, 44, 8140–8143, 2010.
- Lana, A., Bell, T. G., Simó, R., Vallina, S. M., Ballabrera-Poy, J., Kettle, A.-J., Dachs, J., Bopp, L., Saltzman, E. S., Stefels, J., Johnson, J. E., and Liss, P. S.: An updated climatology of surface ocean dimethylsulphide concentrations and emission fluxes in the global ocean, *Global Biogeochem. Cy.*, 25, GB1004, doi:10.1029/2010GB003850, 2011.
- Lee, P. A., Rudisill, J. R., Neeley, A. R., Hutchins, D. A., Feng, Y., Hare, C. E., Leblanc, K., Rose, J. M., Wilhelm, S., and Rowe, J. M.: Effects of increased pCO₂ and temperature on the North Atlantic Spring Bloom: III. Dimethylsulfoniopropionate, *Mar. Ecol. Prog. Ser.*, 388, 41–419, 2009.
- Liu, J., Weinbauer, M. G., Maier, C., Dai, M., and Gattuso, J.-P.: Effect of ocean acidification on microbial diversity and on microbe-driven biogeochemistry and ecosystem functioning, *Aquat. Microb. Ecol.*, 61, 291–305, 2010.
- Marie, D., Brussaard, C. P. D., Partensky, F., and Vaulot, D.: Enumeration of phytoplankton, bacteria and viruses in marine samples, in: *Current protocols in cytometry*, edited by: Robinson, J. P., Darzynkiewicz, Z., Dean, P. N., Rabinovitch, P. S., Stewart, C. C., Tanke, H. J., and Wheless, L. L., John Wiley and Sons, 11.11.11–11.11.15, 1999.
- Meakin, N. G. and Wyman, M.: Rapid shifts in picoeukaryote community structure in response to ocean acidification, *ISME J.*, 5, 1397–1405, 2011.
- Moran, M. A., Reisch, C. R., Kiene, R. P., and Whitman, W. B.: Genomic insights into bacterial DMSP transformations, *Annu. Rev. Mar. Sci.*, 4, 523–542, 2012.
- Newbold, L. K., Oliver, A. E., Booth, T., Tiwari, B., DeSantis T., Maguire, M., Andersen, G., van der Gast, C. J., and Whiteley, A. S.: The response of marine picoplankton to ocean acidification, *Environ. Microbiol.*, 14, 2293–2307, 2012.
- Piontek, J., Borchard, C., Sperling, M., Schulz, K. G., Riebesell, U., and Engel, A.: Response of bacterioplankton activity in an Arctic fjord system to elevated pCO₂: results from a mesocosm perturbation study, *Biogeosciences*, 10, 297–314, doi:10.5194/bg-10-297-2013, 2013.
- Polimene, L., Archer, S. D., Butenschön, M., Allen, J. I.: A mechanistic explanation for the Sargassa Sea DMS “summer paradox”, *Biogeochemistry*, 110, 243–255, 2012.
- Rap, A., Scott, C. E., Spracklen, D. V., Bellouin, N., Forster, P. M., Carslaw, K. C., Schmidt, A., and Mann, G.: Natural aerosol direct and indirect radiative effects, *Geophys. Res. Lett.*, 40, 3297–3301, 2013.
- Raven, J. A., Caldeira, K., Elderfield, H. E., Hoegh-Guldberg, O., Liss, P. S., Riebesell, U., Shepherd, J., Turley, C., and Watson, A.: Ocean acidification due to increasing atmospheric carbon dioxide, Royal Society, London, UK, 2005.

- Rees, A. P., Joint, I., and Donald, K. M.: Early spring bloom phytoplankton-nutrient dynamics at the Celtic Sea Shelf Edge, *Deep-Sea Res. I*, 46, 483–510, 1999.
- Richier, S., Achterberg, E. P., Dumousseaud, C., Poulton, A. J., Suggett, D. J., Tyrrell, T., Zubkov, M. V., and Moore, C. M.: Carbon cycling and phytoplankton responses within highly-replicated shipboard carbonate chemistry manipulation experiments conducted around Northwest European Shelf Seas, *Biogeosciences Discuss.*, 11, 3489–3534, doi:10.5194/bgd-11-3489-2014, 2014a.
- Richier, S., Achterberg, E. P., Archer, S., Bretherton, L., Brown, I., Clark, D., Dumousseaud, C., Holland, R. J., Hopkins, F. E., MacGilchrist, G. A., Moore, C. M., Poulton, A., Rees, A., Shi, T., Stinchcombe, M., Suggett, D., Zubkov, M. V., Young, J., and Tyrrell, T.: Ocean acidification impacts on sea surface biology and biogeochemistry in Northwest European Shelf Seas: a high-replicated shipboard approach, *British Oceanographic Data Centre – Natural Environment Research Council, UK*, 2014b.
- Riebesell, U. and Tortell, P. D.: Effects of ocean acidification on pelagic organisms and ecosystems, in: *Ocean Acidification*, edited by: Gattuso, J.-P. and Hansson, L., Oxford University Press, 99–121, 2011.
- Simó, R., Pedrós-Alió, C., Malin, G., and Grimalt, J. O.: Biological turnover of DMS, DMSP and DMSO in contrasting open-sea waters, *Mar. Ecol. Prog. Ser.*, 203, 1–11, 2000.
- Simó, R., Archer, S. D., Pedrós-Alió, C., Gilpin, L., and Stelfox-Widdicombe, C. E.: Coupled dynamics of dimethylsulfoniopropionate and dimethylsulphide cycling and the microbial food web in surface waters of the North Atlantic, *Limnol. Oceanogr.*, 47, 53–61, 2002.
- Simó, R.: From cells to globe: approaching the dynamics of DMS(P) in the ocean at multiple scales, *Can. J. Fish. Aquat. Sci.*, 61, 673–684, 2004.
- Six, K. D., Kloster, S., Ilyina, T., Archer, S. D., and Zhang, K.: Global warming amplified by reduced sulphur fluxes as a result of ocean acidification, *Nature Clim. Change*, 3, 975–978, 2013.
- Spielmeyer, A. and Pohnert, G.: Influence of temperature and elevated carbon dioxide on the production of dimethylsulfoniopropionate and glycine betaine by marine phytoplankton, *Mar. Environ. Res.*, 73, 62–69, 2012.
- Stefels, J.: Physiological aspects of the production and conversion of DMSP in marine algae and higher plants, *J. Sea Res.*, 43, 183–197, 2000.
- Stefels, J., Steinke, M., Turner, S., Malin, G., and Belviso, S.: Environmental constraints on the production and removal of the climatically active gas dimethylsulphide (DMS) and implications for ecosystem modelling, *Biogeochemistry*, 83, 245–275, 2007.
- Stefels, J., Dacey, J. W. H., and Elzenga, T. M.: In vivo DMSP-biosynthesis measurements using stable-isotope incorporation and proton-transfer-reaction mass spectrometry (PTR-MS), *Limnol. Oceanogr. Meth.*, 7, 595–611, 2009.
- Steinke, M., Malin, G., Turner, S., and Liss, P. S.: Determinations of dimethylsulfoniopropionate (DMSP) lyase activity using headspace analysis of dimethyl sulphide (DMS), *J. Sea Res.*, 43, 233–244, 2000.
- Sunda, W., Kieber, D. J., Kiene, R. P., and Huntsman, S.: An antioxidant function for DMSP and DMS in marine algae, *Nature*, 418, 371–320, 2002.
- Sunda, W. G., Hardison, R., Kiene, R. P., Bucciarelli, E., and Harada, H.: The effect of nitrogen limitation on cellular DMSP and DMS release in marine phytoplankton: climate feedback implications, *Aquat. Sci.*, 69, 341–351, 2007.
- Todd, J. D., Rogers, R., Li, Y. G., Wexler, M., Bond, P. L., Sun, L., Curson, A. R. J., Malin, G., Steinke, M., and Johnston, A. W. B.: Structural and regulatory genes required to make the gas dimethyl sulfide in bacteria, *Science*, 315, 666–669, 2007.
- Todd, J. D., Curson, A. R. J., Dupont, C. L., Nicholson, P., and Johnston, A. W. B.: The dddP gene, encoding a novel enzyme that converts dimethylsulfoniopropionate into dimethyl sulfide, is widespread in ocean metagenomes and marine bacteria and also occurs in some Ascomycete fungi, *Environ. Microb.*, 11, 1376–1385, 2009.
- Toole, D. A. and Siegel, D. A.: Light-driven cycling of dimethylsulphide (DMS) in the Sargasso Sea: Closing the loop, *Geophys. Res. Lett.*, 31, L09308, doi:10.1029/2004GL019581, 2004.
- Toole, D. A., Kieber, D. J., Kiene, R. P., Siegel, D. A., and Nelson, N. B.: Photolysis and the dimethylsulfide (DMS) summer paradox in the Sargasso Sea, *Limnol. Oceanogr.*, 48, 1088–1100, 2003.
- Toole, D. A., Slezak, D., Kiene, R. P., Kieber, D. J., and Siegel, D. A.: Effects of solar radiation on dimethylsulphide cycling in the western Atlantic Ocean, *Deep-Sea Res. I*, 53, 136–153, 2006.
- Vila-Costa, M., Kiene, R. P., and Simó, R.: Seasonal variability of the dynamics of dimethylated sulfur compounds in a coastal northwest Mediterranean site, *Limnol. Oceanogr.*, 53, 198–211, 2008.
- Vogt, M., Steinke, M., Turner, S., Paulino, A., Meyerhöfer, M., Riebesell, U., LeQuéré, C., and Liss, P.: Dynamics of dimethylsulphoniopropionate and dimethylsulphide under different CO₂ concentrations during a mesocosm experiment, *Biogeosciences*, 5, 407–419, doi:10.5194/bg-5-407-2008, 2008.
- Weinbauer, M. G., Mari, X., and Gattuso, J.-P.: Effect of ocean acidification on the diversity and activity of heterotrophic marine microorganisms, in: *Ocean Acidification*, edited by: Gattuso, J.-P. and Hansson, L., Oxford University Press, 99–121, 2011.
- Wingenter O. W., Haase K. B., Zeigler M., Blake D. R., Rowland F. S., Sive B. C., Paulino A., Runar T., Larsen A., Schulz K., Meyerhofer M., and Riebesell U.: Unexpected consequences of increasing CO₂ and ocean acidity on marine production of DMS and CH₂ClI: Potential climate impacts, *Geophys. Res. Lett.*, 34, L05710, doi:10.1029/2006GL028139, 2007.
- Wolfe, G. V., Levasseur, M., Cantin, G., and Michaud, S.: Microbial consumption and production of dimethyl sulfide (DMS) in the Labrador Sea, *Aquat. Microb. Ecol.*, 18, 197–205, 1999.
- Zubkov, M. V., Fuchs, B. M., Archer, S. D., Kiene, R. P., Amann, R., and Burkhill, P. H.: Rapid turnover of dissolved DMS and DMSP by defined bacterioplankton communities in the stratified euphotic zone of the North Sea, *Deep-Sea Res. II*, 49, 3017–3038, 2002.
- Zubkov, M., Linn, L. J., Amann, R., and Kiene, R. P.: Temporal patterns of biological dimethylsulphide (DMS) consumption during laboratory-induced phytoplankton bloom cycles, *Mar. Ecol. Prog. Ser.*, 271, 77–86, 2004.